Transport experiments in Alcator-C-Mod*

M. Greenwald,† R. L. Boivin, P. Bonoli, C. Christensen, C. Fiore, D. Garnier, J. Goetz, S. Golovato, M. Graf, R. Granetz, S. Horne, T. Hsu, A. Hubbard, I. Hutchinson, J. Irby, C. Kurz, B. LaBombard, B. Lipschultz, T. Luke, E. Marmar, G. McCracken, A. Niemczewski, P. O'Shea, M. Porkolab, J. Rice, J. Reardon, J. Schachter, J. Snipes, P. Stek, Y. Takase, J. Terry, M. Umansky, R. Watterson, and S. Wolfe
Plasma Fusion Center, Massachusetts Institute of Technology, Cambridge, Massachusetts 02139

F. Bombarda
ENEA-Frascati, Frascati, Italy

M. May
Johns Hopkins University, Baltimore, Maryland 21218

B. Welch
University of Maryland, College Park, Maryland 20742

(Received 14 November 1994; accepted 17 February 1995)

A series of transport experiments has been carried out in Alcator-C-Mod. [Phys Plasmas **1**, 1511 (1994)]. Data from both Ohmic and ICRF (ion cyclotron range of frequencies) heated plasmas can be fitted with an L-mode (low mode) scaling law. The Ohmic τ_E's show no scaling with density in any regime and can reach values of 2–3 times neo-Alcator. Impurity confinement has been studied with the laser blow-off technique with τ_I showing nearly linear scaling with plasma current. Ohmic and ICRF H modes are obtained over a wide range of discharge parameters, extending the range in the international database for nB, by almost a factor of 10. The power threshold for ELM-free (edge localized mode) discharges is in rough agreement with the scaling $P/S=0.044nB$. Energy diffusivities of Ohmic and ICRF heated plasmas have been measured from local analysis of plasma profiles and power fluxes. The same analysis produces a value for plasma resistivity which lies between the Spitzer and neoclassical calculations. Analysis of plasma transients have yielded values for particle diffusivity and convection velocity. © *1995 American Institute of Physics.*

I. INTRODUCTION

The Alcator-C-Mod[1] tokamak is a compact high field device capable of producing shaped diverted plasmas. It has a major radius of 0.67 m, a minor radius of 0.21 m, and is designed to operate at toroidal fields up to 9 T, plasma current up to 3 MA, κ up to 1.8, and ICRF (ion cyclotron range of frequencies) heating power to 8 MW. All of the plasma facing components are made of molybdenum with no special wall coating or treatment. Confinement studies have been carried out in hydrogen and deuterium plasmas with $0.35<I_p$ (MA)<1.05; $3.5<B_T$(T)<5.4; $0.20<a$(m)<0.24; $0.65<R$(m)<0.70; $0.7<n_e(10^{20}\ \mathrm{m}^{-3})<2.4$; $1.1<\kappa<1.6$; $0<P_{\mathrm{ICRF}}$ (MW)<1.8. The Z_{eff} is low, typically <1.5 for $n_e>1.5\times10^{20}$.

II. GLOBAL ENERGY TRANSPORT STUDIES

The set of diagnostics available for transport studies on C-Mod includes electron cyclotron emission (ECE) for measuring electron temperature profiles, $T_e(r,t)$; a two-color interferometer for determining $n_e(r,t)$; an array of high resolution x-ray spectrometers for measuring $T_i(r,t)$; neutron emission diagnostics for determining $T_i(0,t)$; a visible bremsstrahlung array for measuring $Z_{\mathrm{eff}}(r,t)$; a bolometer array for measuring radiated power profiles, $P_{\mathrm{rad}}(r,t)$; various spectrometers for determining impurity content; and a full set of magnetic diagnostics for calculating the MHD (magnetohydrodynamic) equilibrium and related quantities. The plasma stored energy is calculated by integration of the density and temperature profiles (W_{kin}) and by analysis of the equilibrium with the EFIT (equilibrium FIT) code[2] (W_{MHD}). These generally agree to within 20%; however, for ICRF plasmas, W_{MHD} is systematically higher than W_{kin}. This systematic difference is probably attributable to energy in the minority ion tail. When "no plasma" shots are available for subtraction of stray field effects, we can also obtain the stored energy by analysis of the diamagnetic loop signals. These are in good agreement with W_{MHD}. Shots for confinement analysis were chosen with "standard" criteria: quasi-steady state, sawtoothing, and nondisruptive.

Much of the data taken for the scaling studies described below were obtained as the machine and its subsystems were brought on line. Relatively few dedicated parameter scans were performed. While a fairly large range in operating parameters was obtained, the full multidimensional space available to us was not explored. This is summarized in Table I which gives the average, standard deviation, and correlation matrix for eight independent variables. From the table we see "natural correlations" such as that between I_p and κ or between I_p and P_{in} for the Ohmic plasma, as well as "accidental correlations" such as that between κ and ion mass which are simply the result of not running in all of the available operating space. Note that total input power is necessarily

*Paper 9IB1, Bull. Am. Phys. Soc. 39, 1751 (1994).
†Invited speaker.

 1070-664X/95/2(6)/2308/6/$6.00

TABLE I. Correlation matrix, giving the mean, range and correlations for the independent variables in our data set. Note the "natural correlations" such as that between I_p and κ or between I_p and P_{in} for the Ohmic plasma, as well as "accidental correlations" such as that between κ and ion mass which are simply the result of not running in all of the available operating space.

	$\ln(R)$	$\ln(R/a)$	$\ln(I_p)$	$\ln(B_T)$	$\ln(M)$	$\ln(n_e)$	$\ln(\kappa)$	$\ln(P_{tot})$
mean	−0.38	1.13	−0.41	1.64	0.59	0.13	0.37	0.07
sigma	0.014	0.024	0.27	0.063	0.25	0.36	0.084	0.54
$\ln(R)$	1.00							
$\ln(R/a)$	−0.28	1.00						
$\ln(I_p)$	0.27	−0.13	1.00					
$\ln(B_T)$	−0.09	0.14	0.45	1.00				
$\ln(M)$	0.26	0.10	0.65	0.35	1.00			
$\ln(n_e)$	0.18	0.06	0.73	0.47	0.41	1.00		
$\ln(\kappa)$	0.54	0.22	0.52	0.13	0.63	0.29	1.00	
$\ln(P_{tot})$	−0.01	−0.19	0.72	0.42	0.44	0.64	0.22	1.00

well correlated with ion mass since our main ICRF heating scheme is hydrogen minority in deuterium majority. The table also quantifies our limited range in R, a, and B_T.

A. Ohmic L mode

Contrary to our expectations, stored energy in the Ohmic plasmas increased with I_p but not with n_e. For most discharges, the measured τ_E is greater than the neo-Alcator value.[3] The increase in stored energy with I_p suggested an L-mode (low mode) behavior; a linear regression can be performed to calculate the best fit to a power-law scaling for the data. The range of some parameters (a,R,B_T) in our database is too limited to include in the regression, however, significant results were obtained by fitting against I_p, P_{in}, n_e, and amu (effective ion mass). The results, which include data for ICRF plasmas, are shown in Fig. 1. The coefficients are not distinguishable from ITER89-P[4] (the International Thermonuclear Experimental Reactor) within the error bars of the two fits. Our conclusion is that our Ohmic confinement is following an L-mode-like scaling which for low densities and high currents can exceed neo-Alcator by as much as a factor of 3.[5]

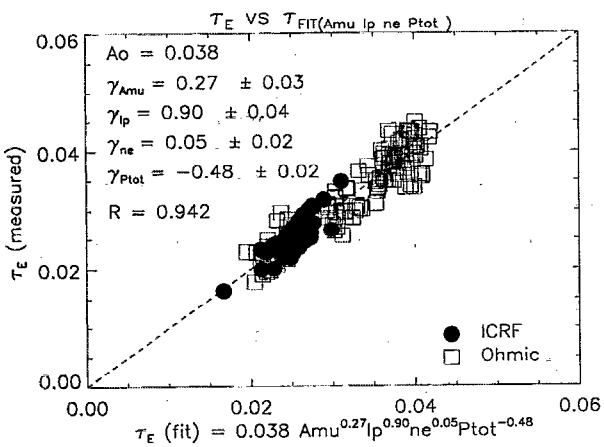

FIG. 1. The measured τ_E for both Ohmic and ICRF heating plasmas is plotted against the best fit to a power-law scaling expression. The gamma's are the power-law scaling coefficients. The result is very close to the ITER89-P equation.[5]

B. ICRF heating and confinement

ICRF heating was performed using a dipole antenna (two current straps spaced toroidally and driven out of phase) with up to 1.8 MW of power at 80 MHz.[6] The heating scenario was hydrogen minority in deuterium at B_T=5.3 T. Antenna loading was 3–25 Ω, increasing with plasma density and decreasing with antenna–plasma spacing. Efficient heating was observed, roughly doubling electron and ion temperatures at the higher RF (radio frequency) powers. There were substantial variations in the relative temperature increase of the electrons and the ions; the best results at current power levels being ΔT_e=1.4 keV and ΔT_i=1.3 keV. The minority concentration deduced from analysis of the Hα/Dα lines, was typically 2%–3%.

Traces of $T_e(0)$ and $T_i(0)$ versus time are shown in Fig. 2. The electron and ion temperatures are strongly modulated by sawtooth activity. The sawtooth period increases by factors of 2–4 over otherwise similar Ohmic plasmas. TRANSP[7] calculations (discussed in the following section) indicate that $q(0)$ drops from ~0.8 to ~0.6 as the RF stabilizes the sawteeth. Despite a small increase in density and Z_{eff}, P_{rad}/P_{in} is unchanged; Z_{eff} shows the same scaling with density and input power for both Ohmic and RF discharges (Fig. 3). For a typical ICRF plasma, with P_{RF}=1.8 MW, I_p=0.8 MA, and

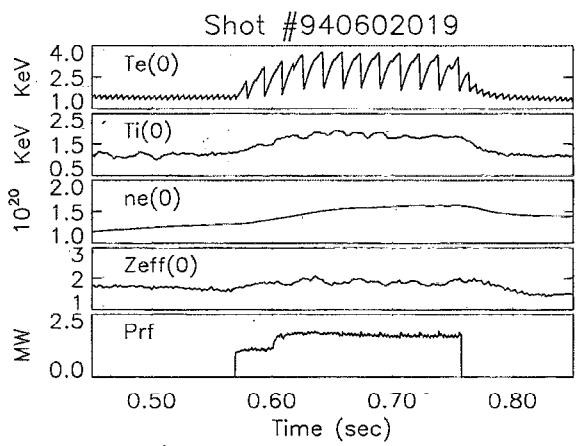

FIG. 2. Traces of plasma temperatures, density, Z_{eff} and P_{ICRF} for a typical ICRF heated discharge.

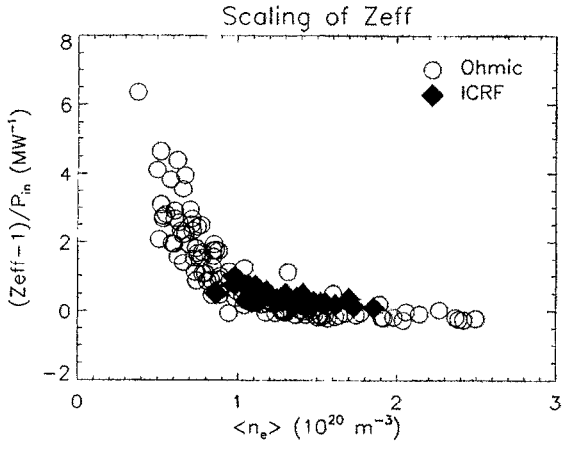

FIG. 3. $[Z_{eff}(0)-1]/P_{in}$ versus line averaged density. At densities above 1.5×10^{20}, Z_{eff} is near 1 for all powers up to 2 MW.

$n_e=1\times10^{20}$, the calculations show that more than 90% of net RF power is absorbed and thermalized; 80% of which is absorbed within $r/a=0.5$, creating an ion tail with approximately 15–20 kJ out of a total stored energy of 60 kJ. This is in quantitative agreement with measurements of ΔW from kinetics, MHD, and diamagnetism as shown in Fig. 4. The energy confinement follows an L-mode-like scaling as demonstrated in Fig. 1.

III. LOCAL TRANSPORT STUDIES

To calculate local transport quantities we have used the TRANSP[7] code. This code uses measured plasma profiles as inputs then calculates the electron and ion heat balance, particle balance, and magnetic diffusion with a fixed boundary equilibrium. For ICRF heated plasmas, the full wave SPRUCE[8] code linked to the Fokker–Planck solver FPPRF[9] is used to calculate the heating power to ions and electrons. For the Ohmic shots at $I_p=0.8$ MA, $n_e=1\times10^{20}$, we have found $\chi_e(a/2)\sim0.2$–0.8 m^2/s. At low densities, where electron and ion transport can be separated, $\chi_i\sim\chi_e$ and is mildly

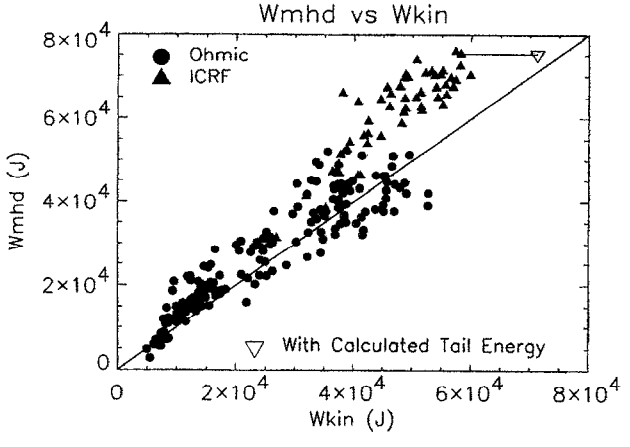

FIG. 4. W_{MHD} vs W_{kin} for the confinement database. These are in good agreement for the Ohmic data. The discrepancy in the higher power ICRF data is likely due to energy stored in the ion tail. W_{MHD} vs $W_{kin}+W_{tail}$ is shown for one case calculated with FPPRF.

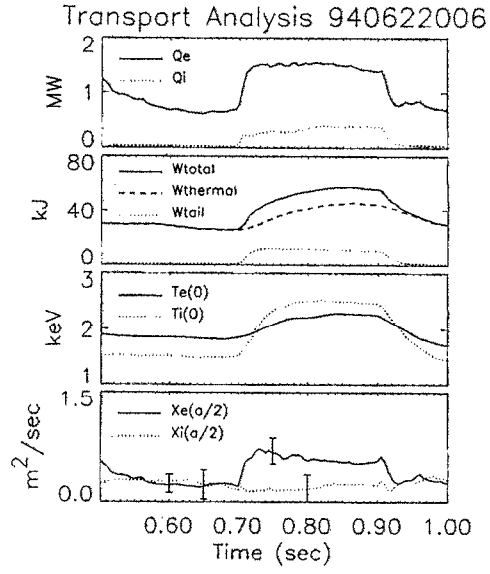

FIG. 5. Heating power, temperatures, stored energies, and thermal diffusivities of the plasma electrons and ions as calculated by TRANSP. During the Ohmic phase $\chi_e\sim\chi_i$ but when the ICRF is applied, χ_e rises to about 1.0 m^2/s with apparently little change in χ_i.

anomalous with $\chi_i/\chi_{neo}=1$–3 with large uncertainties. Figure 5 shows the time evolution of plasma temperatures, stored thermal and tail energies, electron and ion heating powers, and electron and ion diffusivities for a typical ICRF plasma. In this case, χ_e rises to about 1.0 m^2/s with apparently little change in χ_i.

Electrical resistivity, like other parallel transport quantities, is usually measured to be near its classical value. Corrections for trapped particles and related effects are embodied in the neoclassical theory.[10] Experiments on other machines have found values ranging from classical[11] to neoclassical[12] and in between.[13] For C-Mod we have investigated this issue by using TRANSP to solve the poloidal field diffusion equation with I_p, $T_e(r,t)$, $Z_{eff}(r,t)$ as inputs. The code calculates the evolution of the current profile and parallel electric field. The calculated surface voltage is then compared to the value measured with our magnetic diagnostic set. The results are shown in Fig. 6 where the surface voltage calculated with the neoclassical model and the Spitzer model are both plotted against the measured surface voltage. Data for the "correct" model would fall on the slope=1 line. Instead, data from both models straddle this line, indicating that our resistivity values fall in between the calculations of the two models. Errors for this calculation include uncertainties in the measured temperature and density profiles, calibration of the visible bremsstrahlung, and very small errors in quantities calculated from the magnetic reconstruction. Overall, we estimate the uncertainty in the resistivity calculation to be in the range 20%–30%. We note that at higher collisionalities our results converge on $\eta_{measured}=\eta_{Spitzer}=\eta_{neoclassical}$ as expected.

IV. H MODE

Ohmic ELM-free (edge localized modes) H modes (high mode) were first achieved by ramping down the toroidal field

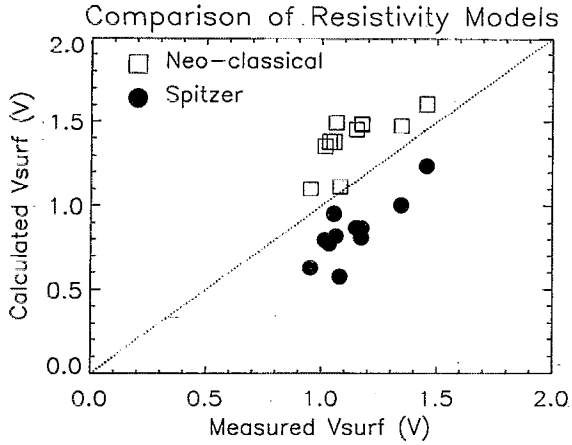

FIG. 6. Values of the plasma surface voltage, V_{surf}, calculated with TRANSP with the Spitzer and neoclassical resistivity models is plotted against the measured V_{surf}. Our results indicate resistivity somewhere in between the two calculations.

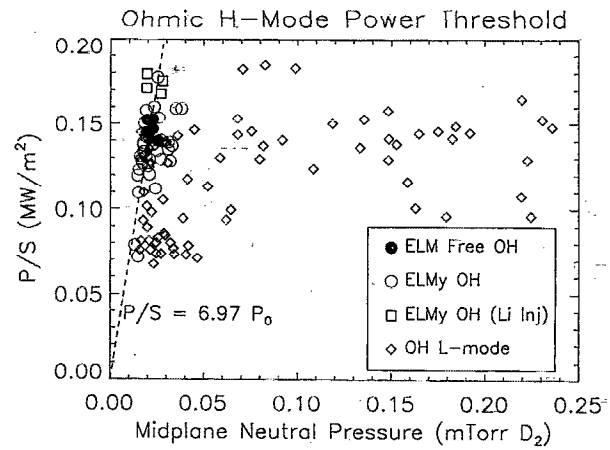

FIG. 7. Surface power density, P/S, plotted against midplane neutral pressure, P_0, for Ohmic L-mode and H-mode discharges. The Ohmic H-mode discharges have the lowest values of P_0 in the database.

at constant plasma current, I_p=0.65 MA, and moderate density, n_e=1.0×10^{20} m^{-3}, with the grad-B drift toward the single null divertor.[14] The H-mode transitions occurred with $3.0<B_T<3.3$ at an Ohmic power of about 1 MW and were followed by a rapid density rise for up to 50 ms before the plasma either returned to L mode or disrupted at about q=2. Estimates of the energy confinement time, not including dW/dt corrections (which can be as much as 60% of the input power), are between 40 and 60 ms, which is in the range of the ITER[15] H-mode scaling.[16] H-mode enhancement factors for energy confinement and global particle confinement are typically about 2 above L mode. At higher toroidal field, up to 5.3 T, ELMy Ohmic H modes have been observed as the toroidal field starts to ramp down at the end of a discharge or during the flattop following the injection of lithium pellets. While these H modes had longer durations (up to 350 ms), the increases in the density and stored energy were typically about 20% due to the rapid (5–6 kHz) ELMs. However, for the best of these shots, the H-mode enhancement factor can be as high as 1.5.

ICRF heating has also been used to achieve H modes with up to 1.5 MW of additional power. The equilibria, while nearly single null diverted plasmas, were in fact marginally limited. ELM-free H modes of 10–15 ms duration and ELMy H modes of up to 50 ms duration have been observed during ICRH at constant toroidal field of 5.3 T with densities in the range of $1.2<n_e<1.8\times10^{20}$ m^{-3}. The duration of these H modes is often limited by the reduced coupling of the RF power due to reduced loading resistance during the H mode. The drop in power makes it more difficult to maintain the H mode. A feedback system on the RF frequency and/or plasma position will be implemented in the future to maintain good coupling through the changes in the edge plasma at the L–H transitions. The particle confinement again doubles during the H mode, but the improvement in energy confinement is difficult to quantify due to the short duration and change in RF power during these H modes.

The H-mode power threshold observed in C-Mod is in good agreement with the ITER scaling,[17] P/S (MW/m^2) $=0.044nB$ (10^{20} m^{-3} T) for ELM-free discharges, while the ELMy H modes tend to have a significantly lower threshold power. However, considering both sets of data, there is no clear dependence on n_e or B_T. No special wall conditioning techniques were necessary to achieve most of these H modes, though the lowest power threshold ELMy H modes were obtained after injecting lithium pellets into the plasma, which may have helped condition the plasma facing components. Note that the first wall is composed of all molybdenum tiles and the ICRF antenna Faraday shields and protection tiles are made of molybdenum which have been coated with titanium carbide. The present results extend the international database for the H-mode threshold up to values of P/S=0.33 MW/m^2 and $nB>9\times10^{20}$ m^{-3} T, which are in the expected range for ITER.

By comparing the parameters in a time-slice database of Ohmic H-mode discharges and Ohmic L-mode discharges, an attempt was made to determine what were the most important characteristics that may have helped to achieve H mode. The parameters considered were the inner and outer gap, lower triangularity, midplane neutral pressure, Z_{eff}, and the input power density, P/S. While the statistics are somewhat limited, the strongest apparent dependence of the threshold for well-diverted discharges (which presently includes only Ohmic H modes) is on the midplane neutral pressure, P_0. The H modes fall on a line with $P/S\sim P_0$, representing the minimum in neutral pressure for both L- and H-mode deuterium discharges. Figure 7 shows the input power density versus P_0 for L-mode and Ohmic H-mode discharges. The H-mode discharges have lower midplane neutral pressure than almost all of the L-mode discharges. For the ICRF heated plasmas, the midplane neutral pressure was high in both L-mode and H-mode discharges, perhaps because of the requirement to run the plasma near the outboard limiter and antenna to obtain good RF coupling.

V. IMPURITY CONFINEMENT

Impurity particle confinement has been measured using the laser blow-off technique.[18] Trace amounts (about 3×10^{17}

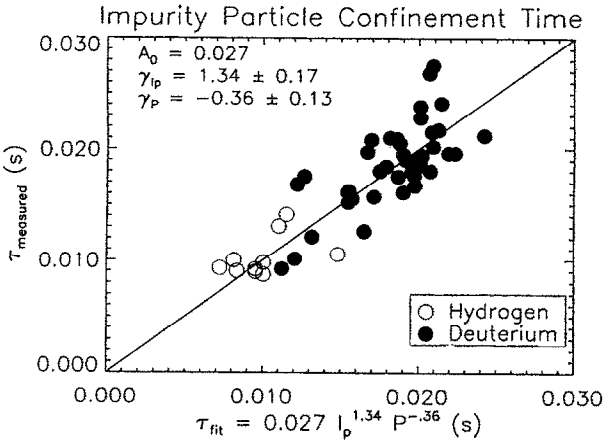

FIG. 8. Impurity confinement times plotted against a power-law fit. The dominant scaling is a nearly linear dependence on I_p.

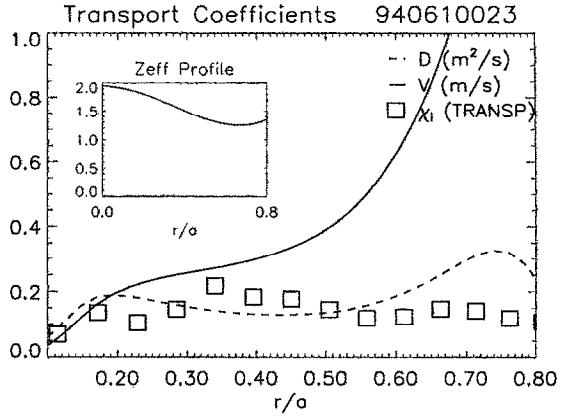

FIG. 9. Profiles of particle diffusivity $D(r)$ and convective velocity $V(r)$ calculated by from the plasma response to a set of gas puffs. The inset graph shows a typical Z_{eff} profile from the same shot.

atoms) of nonrecycling impurities are ablated from a 1 μm thick target located about 1 m from the plasma using a 2 J, 30 ns Q-switched ruby laser pulse and are injected at the horizontal midplane. The spatial and temporal evolution of these impurities is observed with a number of spectroscopic diagnostics in the x-ray, VUV (vacuum ultraviolet), and visible regions of the spectrum. Typically, observations of central charge states show a very fast rise time (few milliseconds) as the impurities are transported inwards. This is followed by a nearly exponential decay as the impurities diffuse out of the plasma. The decay time is used to characterize the impurity particle confinement time.

Scaling studies have been conducted to measure this time as a function of various plasma parameters. It was found that the confinement time scales almost linearly with plasma current, although the range in B_T is insufficient to distinguish between a current and a q scaling. The observed dependence on electron density and mass of the working gas was found to be weak. This result is summarized in Fig. 8. No dependence on Z_{eff} of the plasma or Z of the injected impurity (in the range from 13 to 42) was observed. Impurity transport coefficients have been deduced on the basis of these times and measured impurity emissivity profiles. Anomalous diffusion coefficients of about 0.4–0.7 m^2/s and convective velocities of about 2.0–3.5 m/s at the edge are consistent with observed measurements. These are somewhat higher than the corresponding transport coefficients for the majority species.

VI. TRANSIENT TRANSPORT EXPERIMENTS

A series of gas modulation experiments has been performed to measure core particle transport. The gas flow is modulated at 10 Hz with the amplitude adjusted to produce approximately 5% variations in the line integral density as measured by an interferometer. The density perturbations were observed with the visible bremsstrahlung array. This array has 30 channels, views tangentially on the midplane, and covers from R=0.60 to 0.90 m. with 1 cm chordal resolution. The array is filtered to look at continuum at 536 nm; the signal is usually dominated by free–free bremsstrahlung. By assuming toroidal symmetry, standard Abel inversion techniques can be applied to get the local emissivity profile ($\sim n_e^2 Z_{\text{eff}}/T_e^{0.37}$) from the measured brightness profile. Then assuming that the Z_{eff} profile is flat (this assumption should be best when Z_{eff} is close to 1) we can calculate a "pseudo density" profile using the measured emissivity and T_e profiles. While this profile is only qualitatively correct, the transport coefficients D and V depend mainly on the timing and relative amplitude of changes across the profile. The visible bremsstrahlung signals with their excellent spatial and temporal resolution are well suited for these purposes; $D(r)$ and $V(r)$ are obtained by solving in a least-squares sense:

$$\frac{1}{r}\frac{\partial}{\partial t}\int \rho n_e \, d\rho = D\frac{\partial n_e}{\partial r} + V n_e . \tag{1}$$

For a typical case (Fig. 9), D is roughly constant and V goes like r; χ_e calculated from power balance was 0.2 m^2/s for this shot giving $\chi_e/D \sim 1$–2. There are no clear trends with plasma density. After divertor detachment,[19] transport appears unchanged; however, following a full poloidal detachment, V increases substantially while D is relatively unchanged. A slightly different analysis can be performed to look at impurity transport when $Z_{\text{eff}} \gg 1$. In some cases, after Li pellet injection where the electron density becomes peaked, impurities accumulate and $Z_{\text{eff}}(0)$ rises to about 7. Assuming the plasma consists of molybdenum plus a background species of charge Z_b, we use the approximation:

$$n_{\text{mo}} = n_e(Z_{\text{eff}} - Z_b)/(Z_{\text{mo}}^2 - Z_{\text{mo}}). \tag{2}$$

Using the same analysis as before, but substituting n_{mo} for n_e, we find that $V(a/2)$ is 30 m/s, over an order of magnitude larger than is typical for electron transport, while D is 0.25 m^2/s about a factor of 2 smaller than electron transport. This result is in quantitative agreement with the neoclassical accumulation of impurities which was also observed following pellet injection on Alcator-C.[20]

VII. SUMMARY

We have found that data from both Ohmic and ICRF heated plasmas can be fitted with an L-mode scaling law. The Ohmic τ_E's show no scaling with density in any regime we have investigated and can reach values of 2–3 times neo-Alcator. Overall, the confinement properties of the Ohmic and ICRF plasmas are apparently distinguished only by the level of input power. Impurity confinement has been studied with the laser blow-off technique and shows a nearly linear scaling with plasma current. The diffusivity for the impurities was in the range 0.4–0.8 m^2/s, somewhat higher than that of the majority species. Analysis of plasma transients have yielded profiles of particle diffusivity and convection velocity; D is typically flat and close to χ_e. Using the TRANSP code and plasma profile data, χ_e and χ_i have been calculated for Ohmic and ICRF heated plasmas. For Ohmic plasmas, $\chi_e(a/2)$ is in the range 0.2–0.8 m^2/s, increasing sharply with the application of RF power. The ion thermal diffusivity is somewhat lower, is typically in the range of $1-3\times\chi_{nc}$ and does not increase with RF power. We also calculate a value for the plasma resistivity which lies between the Spitzer and neoclassical calculations. Ohmic and ICRF H modes are obtained over a wide range of discharge parameters, extending the range in the international database for nB by almost a factor of 10. The power threshold for ELM-free discharges is in rough agreement with the ITER database scaling $P/S=0.044nB$. ELMy H modes were obtained at powers at least a factor of 2 lower than the ELM-free ones. Ohmic H modes are distinguished by having a low midplane neutral pressure.

ACKNOWLEDGMENTS

The authors would like to thank our able and hardworking computer, engineering, and technical staff without whose efforts this research could not have been performed. The authors are also indebted to the developers of the various computer codes cited here.

This work is supported by U.S. Department of Energy Contract No. DE-AC02-78ET51013.

[1]I. Hutchinson, R. Boivin, F. Bombarda, P. Bonoli, S. Fairfax, C. Fiore, J. Goetz, S. Golovato, R. Granetz, M. Greenwald, S. Horne, A. Hubbard, J. Irby, B. LaBombard, B. Lipschultz, E. Marmar, G. McCracken, M. Porkolab, J. Rice, J. Snipes, Y. Takase, J. Terry, S. Wolfe, C. Christensen, D. Garnier, M. Graf, T. Hsu, T. Luke, M. May, A. Niemczewski, G. Tinios, J. Schachter, and J. Urbahn, Phys. Plasmas **1**, 1511 (1994).

[2]L. Lao, H. St. John, R. Stambaugh, A. Kellman, and W. Pfeiffer, Nucl. Fusion **25**, 1611 (1985).

[3]R. Parker, M. Greenwald, S. Luckhardt, E. Marmar, M. Porkolab, and S. Wolfe, Nucl. Fusion **25**, 1127 (1985).

[4]P. Yushmanov, T. Takizuka, K. Riedel, O. Kardaun, J. Cordey, S. Kaye, and D. Post, Nucl. Fusion **30**, 1999 (1990).

[5]M. Greenwald and the Alcator Group, "Confinement of Ohmic and ICRF heated plasmas in Alcator-C-Mod," to appear in *Plasma Physics and Controlled Nuclear Fusion Research*, Proceedings of the 15th International Conference, Seville, 1994 (International Atomic Energy Agency, Vienna, in press).

[6]M. Porkolab and the Alcator Group, in Ref. 5.

[7]R. Hawryluk, *Physics of Plasmas Close to Thermonuclear Conditions*, Proceedings of the Course Held in Varenna, Italy, 1979, edited by B. Coppi (Commission of the European Communities, Brussels, 1980), Vol. 1, p. 19.

[8]D. Smith, P. Colestock, R. Kashuba, and T. Kammash, Nucl. Fusion **27**, 1319 (1987).

[9]G. Hammet, Ph.D. thesis, Princeton University, 1986.

[10]S. P. Hirshman and D. J. Sigmar, Nucl. Fusion **21**, 1079 (1981).

[11]H. Roehr, K. Steuer, and the ASDEX Team, Rev. Sci. Instrum. **59**, 1875 (1988).

[12]M. Zarnstorff, K. McGuire, M. Bell, B. Grek, D. Johnson, D. McCune, H. Park, A. Ramsey, and G. Taylor, Phys. Fluids B **2**, 1852 (1990); M. Kikuchi, M. Azumi, S. Tsuji, K. Tani, and H. Kubo, Nucl. Fusion **30**, 343 (1990).

[13]D. Bartlett, R. Bickerton, M. Brusati, D. Campbell, J. Christiansen, J. Cordey, S. Corti, A. Costley, A. Edwards, J. Fessey, M. Gadeberg, A. Gibson, R. Gill, N. Gottardi, A. Gondhalekar, C. Gowers, F. Hendriks, O. Jarvis, E. Kallne, J. Kallne, S. Kissel, L. De Kock, H. Krause, E. Lazzaro, P. Lo, F. Mast, P. Morgan, P. Nielson, R. Prentice, R. Ross, J. O'Rourke, G. Sadler, F. Schuller, M. Stamp, P. Stott, D. Summers, A. Tanga, A. Taroni, P. Thomas, F. Tibone, G. Tonetti, B. Tubbing, and M. Watkins, Nucl. Fusion **28**, 73 (1988).

[14]J. A. Snipes, R. S. Granetz, M. Greenwald, I. Hutchinson, D. Garnier, J. Goetz, S. Golovato, A. Hubbard, J. Irby, B. Labombard, T. Luke, E. Marmar, A. Niemczewski, P. Stek, Y. Takase, J. Terry, and S. Wolfe, Nucl. Fusion **34**, 1039 (1994).

[15]K. Tomabechi, J. R. Gilleland, Yu. A. Sokolv, R. Toshci, and the ITER Team, Nucl. Fusion **31**, 1135 (1991).

[16]F. Ryter, O. Gruber, O. J. W. F. Kardaun, H. P. Menzler, F. Wagner, D. P. Schissel, J. C. DeBoo, and S. M. Kaye, Nucl. Fusion **33**, 979 (1993).

[17]F. Ryter, O. Gruber, K. Buchl, A. Field, C. Fuchs, O. Gehre, A. Herrmann, M. Kaufmann, W. Koppendorfer, F. Mast, H. Murmann, J. M. Noterdaeme, G. Pereverzev, H. Zohm, and the ASDEX Upgrade Team, *Proceedings of the 20th EPS Conference on Controlled Fusion and Plasma Physics*, 1993, Lisboa, edited by J. Cabral (European Physical Society, Petit-Lancy, 1993), Vol. 17C, Part I, p. I-23.

[18]E. S. Marmar, J. L. Cecchi, and S. Cohen, Rev. Sci. Instrum. **46**, 1149 (1975).

[19]B. Lipschultz, J. Goetz, B. LaBombard, G. M. McCracken, J. L. Terry, M. Graf, R. S. Granetz, D. Jablonski, C. Kurz, A. Niemczewski, and J. Snipes, "Dissipative divertor operation in the Alcator-C-Mod tokamak," to appear in J. Nucl. Mater.

[20]R. Petrasso, J. Hopf, K. Wenzel, D. Sigmar, J. Terry, and M. Greenwald, Phys. Rev. Lett. **57**, 707 (1986).